LECTURE 17: Radiation from Apertures

(*The uniqueness theorem. The equivalence principle. The application of the equivalence principle to aperture problem. The uniform rectangular aperture and the radiating slit. The tapered rectangular aperture.*)

1. Introduction

Aperture antennas constitute a large class of antennas, which emit EM waves through an opening (or aperture). These antennas have close analogs in acoustics, namely, the megaphone and the parabolic microphone. The pupil of the human eye, too, is an aperture receiver for optical radiation. At radio and microwave frequencies, horns, waveguide apertures and slots, reflector antennas, and printed patches or slots are examples of aperture antennas. Aperture antennas are commonly used at UHF and above where their sizes are relatively small. Their gain increases as $\sim f^2$. For an aperture antenna to be efficient and to have high directivity, it must have an area $\geq \lambda^2$. Thus, these antennas tend to be very large at low frequencies.

To facilitate the analysis of these antennas, the equivalence principle is applied. This allows for carrying out the far-field analysis in the outer (unbounded) region only, which is external to the antenna. This requires the knowledge of the tangential field components at the aperture.

2. Uniqueness Theorem

A solution is said to be unique if it is the only one possible among a given class of solutions. The EM field in a region $V_{[S]}$ is unique if

- all sources are given;
- either the tangential $\mathbf{E}_{\tan}$ components or the tangential $\mathbf{H}_{\tan}$ components are specified at the boundary S. [1]

The uniqueness theorem follows from Poynting's theorem in its integral form:

[1] A more general statement of the theorem asserts that any one of the following boundary conditions at S ensure the solution's uniqueness: **(1)** $\mathbf{E}_{\tan}\big|_S$, or **(2)** $\mathbf{H}_{\tan}\big|_S$, or **(3)** $E_{\tan 1}\big|_S$ and $H_{\tan 1}\big|_S$, or **(4)** $E_{\tan 2}\big|_S$ and $H_{\tan 2}\big|_S$. Here, $\mathbf{E}_{\tan} = \mathbf{E} - \mathbf{E}\cdot\hat{\mathbf{n}}$ is the tangential component of $\mathbf{E}$ at the surface S while $E_{\tan 1}$ and $E_{\tan 2}$ are its components. The same notations hold for $\mathbf{H}$.
[N.K. Nikolova, "Electromagnetic boundary conditions and uniqueness revisited," *IEEE Antennas & Propagation Magazine*, vol. 46, no. 5, pp. 141–149, Oct. 2004.]

$$\oiint_S (\mathbf{E}\times\mathbf{H}^*)\cdot d\mathbf{s} + j\omega\iiint_{V_S}(\mu|\mathbf{H}|^2 - \varepsilon|\mathbf{E}|^2)dv + \iiint_{V_S}\sigma|\mathbf{E}|^2\,dv = -\iiint_{V_S}(\mathbf{E}\cdot\mathbf{J}^{i*} + \mathbf{H}^*\cdot\mathbf{M}^i)dv\,. \quad (17.1)$$

We start with the supposition that a given EM problem has two solutions (due to the same sources and the same boundary conditions): $(\mathbf{E}^a, \mathbf{H}^a)$ and $(\mathbf{E}^b, \mathbf{H}^b)$. The difference field is then formed:

$$\begin{cases} \delta\mathbf{E} = \mathbf{E}^a - \mathbf{E}^b, \\ \delta\mathbf{H} = \mathbf{H}^a - \mathbf{H}^b. \end{cases} \quad (17.2)$$

The difference field has no sources; thus, it satisfies the source-free form of (17.1):

$$\oiint_S (\delta\mathbf{E}\times\delta\mathbf{H}^*)\cdot d\mathbf{s} + j\omega\iiint_{V_S}(\mu|\delta\mathbf{H}|^2 - \varepsilon|\delta\mathbf{E}|^2)dv + \iiint_{V_S}\sigma|\delta\mathbf{E}|^2\,dv = 0\,. \quad (17.3)$$

Since both fields satisfy the same boundary conditions, then $\delta\mathbf{E}_{\tan} = 0$ or $\delta\mathbf{H}_{\tan} = 0$ over S, which makes the surface integral in (17.3) zero. This results in

$$\underbrace{j\omega\iiint_{V_S}(\mu|\delta\mathbf{H}|^2 - \varepsilon|\delta\mathbf{E}|^2)dv}_{\text{imaginary}} + \underbrace{\iiint_{V_S}\sigma|\delta\mathbf{E}|^2\,dv}_{\text{real}} = 0, \quad (17.4)$$

which is true only if

$$\begin{cases} \omega\iiint_{V_S}(\mu|\delta\mathbf{H}|^2 - \varepsilon|\delta\mathbf{E}|^2)dv = 0, \\ \iiint_{V_S}\sigma|\delta\mathbf{E}|^2\,dv = 0. \end{cases} \quad (17.5)$$

If we assume some dissipation ($\sigma > 0$), however slight, equations (17.5) are satisfied only if $\delta\mathbf{E} = \delta\mathbf{H} = 0$ everywhere in the volume V_S. This implies the uniqueness of the solution. If $\sigma = 0$ (a common approximation), multiple solutions $(\delta\mathbf{E}, \delta\mathbf{H})$ may exist in the form of resonant modes. However, these resonant modes can be derived using eigenvalue analysis and they are not considered as the particular solution for the given sources. The particular unique solution for the loss-free case can be obtained from a problem where σ is assumed nonzero and then the limit is found as $\sigma \to 0$.

3. Equivalence Principles

The equivalence principle is based on the uniqueness theorem. It allows for the simplification of certain EM problems. As long as a problem is re-formulated so that it preserves the boundary conditions for the original field $(\mathbf{E}_o, \mathbf{H}_o)$ at S, it is going to produce the only one possible solution for the region V_S bounded by S. Such a re-formulated problem is referred to as an ***equivalent problem***.

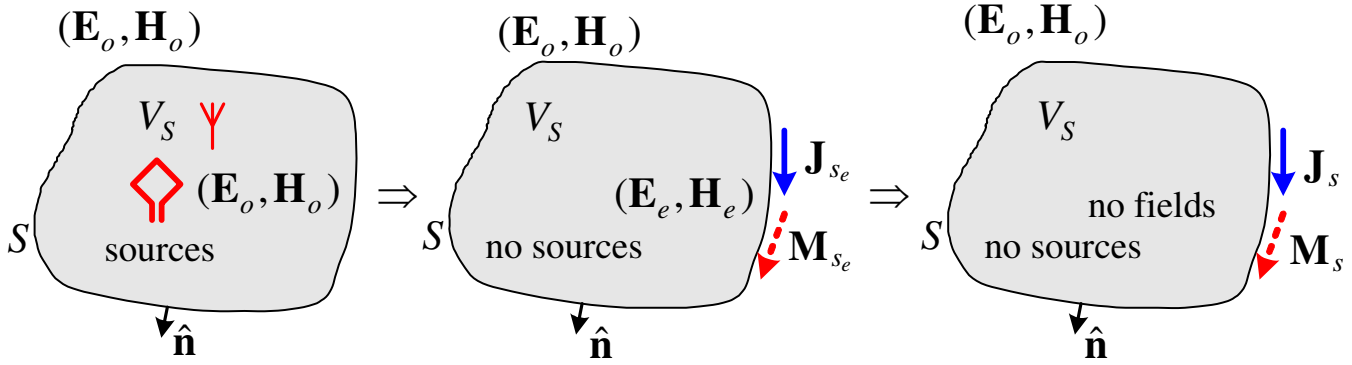

(a) Original problem

(b) General equivalent problem

(c) Equivalent problem with zero fields

The equivalent problem in (b) assumes that the field inside the volume enclosed by S is given by $(\mathbf{E}_e, \mathbf{H}_e)$, which is different from the original field $(\mathbf{E}_o, \mathbf{H}_o)$. This results in a field discontinuity at the surface S, which demands the existence of surface current densities (as per Maxwell's equations):

$$\begin{aligned} \mathbf{J}_{s_e} &= \hat{\mathbf{n}} \times (\mathbf{H}_o - \mathbf{H}_e), \\ \mathbf{M}_{s_e} &= (\mathbf{E}_o - \mathbf{E}_e) \times \hat{\mathbf{n}}. \end{aligned} \tag{17.6}$$

For the equivalent problem in (c), where $(\mathbf{E}_e, \mathbf{H}_e)$ is set to zero, these surface current densities are

$$\begin{aligned} \mathbf{J}_s &= \hat{\mathbf{n}} \times \mathbf{H}_o, \\ \mathbf{M}_s &= \mathbf{E}_o \times \hat{\mathbf{n}}. \end{aligned} \tag{17.7}$$

The zero-field formulation is often referred to as *Love's equivalence principle.* We can apply Love's equivalence principle in three different ways.

(a) We assume that the boundary S is a perfect conductor. As per image theory, in an equivalent open problem, this eliminates the surface electric currents, i.e., $\mathbf{J}_s = 0$, and leaves just surface magnetic currents of double strength $2\mathbf{M}_s$ radiating in free space. This approach is illustrated below.

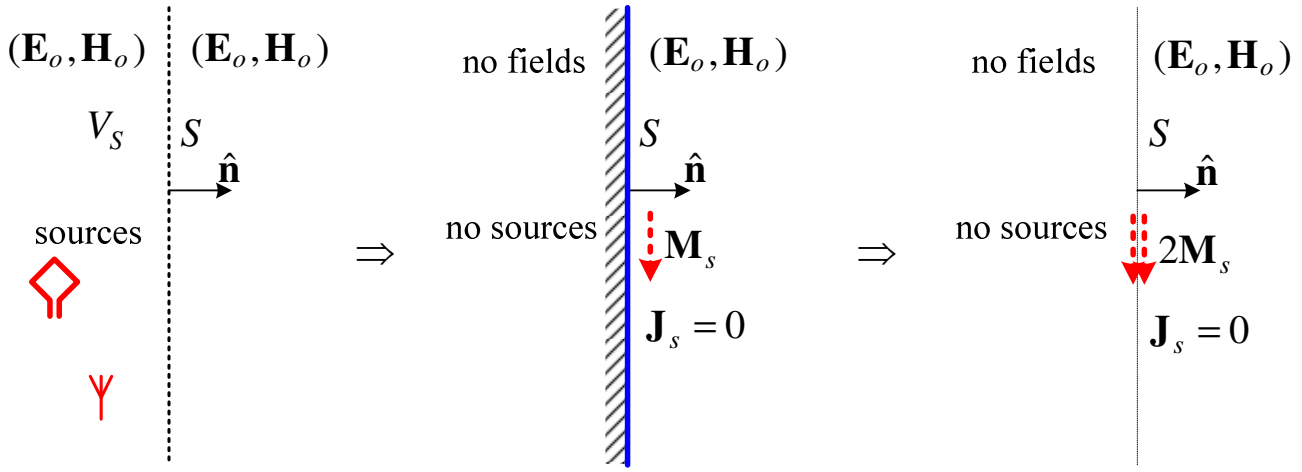

(a) Original problem

(b) Equivalent problem - electric wall

(c) Equivalent problem - images

(b) We assume that the boundary S is a perfect magnetic conductor. In the equivalent image-based problem, the surface magnetic currents are zero, $\mathbf{M}_s = 0$, and the surface electric currents of double strength $2\mathbf{J}_s$ radiate in free space. This approach is illustrated below.

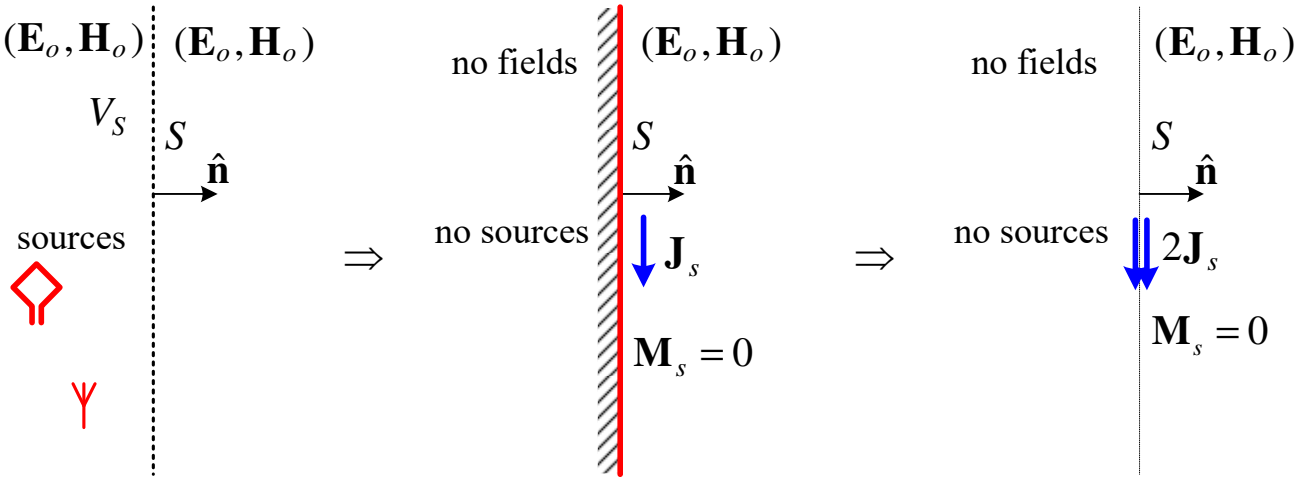

(a) Original problem

(b) Equivalent problem - magnetic wall

(c) Equivalent problem - images

(c) Employ both $\mathbf{J}_s$ and $\mathbf{M}_s$ from (17.7) without any assumptions of fictitious conductors behind them. These equivalent surface-current sources radiate in open space. It can be shown that the radiation from these equivalent currents leads to zero field inside V_S. [See Ewald-Oseen extinction theorem: A. Ishimaru, *Electromagnetic Wave Propagation, Radiation, and Scattering*, Prentice Hall, 1991, p. 173]

The first two approaches are not very accurate in the case of curved boundary surfaces S because the image theory holds only if the curvature radius is large compared to the wavelength. However, in the case of flat infinite planes (walls), the image theory holds exactly, and all three approaches should produce the same external field as per the uniqueness theorem.

The above approaches are used to compute fields in half-space as excited by apertures. The field behind S is assumed known and is used to define the equivalent surface currents. The open-region far-zone solutions for the vector potentials $\mathbf{A}$ (resulting from $\mathbf{J}_s$) and $\mathbf{F}$ (resulting from $\mathbf{M}_s$) are

$$\mathbf{A}(P) = \mu \frac{e^{-j\beta r}}{4\pi r} \iint_S \mathbf{J}_s(\mathbf{r}') e^{j\beta \hat{\mathbf{r}}\cdot\mathbf{r}'} ds', \tag{17.8}$$

$$\mathbf{F}(P) = \varepsilon \frac{e^{-j\beta r}}{4\pi r} \iint_S \mathbf{M}_s(\mathbf{r}') e^{j\beta \hat{\mathbf{r}}\cdot\mathbf{r}'} ds'. \tag{17.9}$$

Here, $\hat{\mathbf{r}}$ denotes the unit vector pointing from the origin of the coordinate system (the center of the aperture) to the point of observation $P(\mathbf{r})$. The source point $Q(\mathbf{r}')$ is at $\mathbf{r}'$. Since in the far zone the field propagates radially away from the antenna, it is convenient to introduce the ***propagation vector*** or ***wave vector***,

$$\boldsymbol{\beta} = \beta \hat{\mathbf{r}}, \tag{17.10}$$

which characterizes both the wave's phase constant β (wavenumber) and its direction of propagation. The far-zone vector potentials can then be written as

$$\mathbf{A}(P) = \mu \frac{e^{-j\beta r}}{4\pi r} \iint_S \mathbf{J}_s(\mathbf{r}') e^{j\boldsymbol{\beta}(\mathbf{r}')\cdot\mathbf{r}'} ds', \tag{17.11}$$

$$\mathbf{F}(P) = \varepsilon \frac{e^{-j\beta r}}{4\pi r} \iint_S \mathbf{M}_s(\mathbf{r}') e^{j\boldsymbol{\beta}(\mathbf{r}')\cdot\mathbf{r}'} ds'. \tag{17.12}$$

The relations between the far-zone field vectors and the vector potentials are

$$\mathbf{E}_A^{\text{far}} = -j\omega(A_\theta \hat{\boldsymbol{\theta}} + A_\varphi \hat{\boldsymbol{\varphi}}), \text{ (due to } \mathbf{A} \text{ only)} \tag{17.13}$$

$$\mathbf{H}_F^{\text{far}} = -j\omega(F_\theta \hat{\boldsymbol{\theta}} + F_\varphi \hat{\boldsymbol{\varphi}}), \text{ (due to } \mathbf{F} \text{ only)}. \tag{17.14}$$

Since

$$\mathbf{E}_F^{\text{far}} = \eta \mathbf{H}_F^{\text{far}} \times \hat{\mathbf{r}}, \tag{17.15}$$

the total far-zone electric field (due to both **A** and **F**) is found as

$$\mathbf{E}^{\text{far}} = \mathbf{E}_A^{\text{far}} + \mathbf{E}_F^{\text{far}} = -j\omega\left[(A_\theta + \eta F_\varphi)\hat{\boldsymbol{\theta}} + (A_\varphi - \eta F_\theta)\hat{\boldsymbol{\varphi}}\right]. \tag{17.16}$$

Equation (17.16) requires both vector potentials, **A** and **F**, as arising from both types of surface currents. Computations are reduced in half if image theory is used in conjunction with an electric or a magnetic wall assumption.

4. Application of the Equivalence Principle to Aperture Problems

The equivalence principle is widely used in the analysis of aperture antennas. To calculate exactly the far field, the exact field distribution at the antenna aperture is needed. In the case of exact knowledge of the aperture field distribution, all three approaches given above produce the same results. However, the aperture field distribution is usually not known exactly and approximations are used. Then, the three equivalence-principle approaches produce slightly different results, the consistency being dependent on how accurate our knowledge about the aperture field is. Often, it is assumed that the field is to be determined in half-space, leaving the feed and the antenna behind an infinite wall *S*. The aperture of the antenna S_A is this portion of *S* where we have an approximate knowledge of the field distribution based on the type of the feed line or the incident wave illuminating the aperture. This is the so-called ***physical optics*** approximation, which is more accurate than the ***geometrical optics*** approach of ray tracing.

Let us assume that the field at the aperture S_A is known: $\mathbf{E}_a, \mathbf{H}_a$, and it is zero everywhere on *S* except at S_A. The equivalent current densities are:

$$\left|\begin{array}{l} \mathbf{J}_s = \hat{\mathbf{n}} \times \mathbf{H}_a, \\ \mathbf{M}_s = \mathbf{E}_a \times \hat{\mathbf{n}}. \end{array}\right. \tag{17.17}$$

The substitution of (17.17) into (17.11) and (17.12) produces

$$\mathbf{A}(P) = \mu \frac{e^{-j\beta r}}{4\pi r} \iint_{S_A} \hat{\mathbf{n}} \times \mathbf{H}_a(\mathbf{r}') \cdot e^{j\boldsymbol{\beta}(\mathbf{r}')\cdot\mathbf{r}'} ds', \tag{17.18}$$

$$\mathbf{F}(P) = -\varepsilon \frac{e^{-j\beta r}}{4\pi r} \iint_{S_A} \hat{\mathbf{n}} \times \mathbf{E}_a(\mathbf{r}') \cdot e^{j\boldsymbol{\beta}(\mathbf{r}')\cdot\mathbf{r}'} ds'. \tag{17.19}$$

We can work with the general vector expression for the far field $\mathbf{E}$ [see (17.16)] written as

$$\mathbf{E}^{\text{far}} = -j\omega\mathbf{A}_{\perp} - j\omega\eta\mathbf{F}\times\hat{\mathbf{r}}, \tag{17.20}$$

where $\mathbf{A}_{\perp}$ contains only the transverse (θ and φ) components of $\mathbf{A}$. Substituting (17.18) and (17.19) into (17.20) yields

$$\mathbf{E}^{\text{far}}(\mathbf{r}) = -j\beta\frac{e^{-j\beta r}}{4\pi r}\hat{\mathbf{r}}\times\iint_{S_A}\left[\hat{\mathbf{n}}\times\mathbf{E}_a(\mathbf{r}') - \eta\hat{\mathbf{r}}\times\left(\hat{\mathbf{n}}\times\mathbf{H}_a(\mathbf{r}')\right)\right]e^{j\boldsymbol{\beta}(\mathbf{r}')\cdot\mathbf{r}'}ds'. \tag{17.21}$$

This is the full vector form of the radiated field resulting from the aperture field, and it is known as the ***vector diffraction integral*** (or ***vector Kirchhoff integral***).

We now consider a practical case of a flat aperture lying in the xy plane with $\hat{\mathbf{n}} \equiv \hat{\mathbf{z}}$. Now, (17.18) and (17.19) simplify as

$$\mathbf{A}(P) = \mu\frac{e^{-j\beta r}}{4\pi r}\hat{\mathbf{z}}\times\iint_{S_A}\mathbf{H}_a(\mathbf{r}')\cdot e^{j\boldsymbol{\beta}(\mathbf{r}')\cdot\mathbf{r}'}ds', \tag{17.22}$$

$$\mathbf{F}(P) = -\varepsilon\frac{e^{-j\beta r}}{4\pi r}\hat{\mathbf{z}}\times\iint_{S_A}\mathbf{E}_a(\mathbf{r}')\cdot e^{j\boldsymbol{\beta}(\mathbf{r}')\cdot\mathbf{r}'}ds'. \tag{17.23}$$

For brevity, the surface integrals in (17.22) and (17.23) are denoted as

$$\mathbf{I}^H = I_x^H\hat{\mathbf{x}} + I_y^H\hat{\mathbf{y}} = \iint_{S_A}\mathbf{H}_a e^{j\boldsymbol{\beta}\cdot\mathbf{r}'}ds', \tag{17.24}$$

$$\mathbf{I}^E = I_x^E\hat{\mathbf{x}} + I_y^E\hat{\mathbf{y}} = \iint_{S_A}\mathbf{E}_a e^{j\boldsymbol{\beta}\cdot\mathbf{r}'}ds'. \tag{17.25}$$

Then,

$$\mathbf{A} = \mu\frac{e^{-j\beta r}}{4\pi r}(-I_y^H\hat{\mathbf{x}} + I_x^H\hat{\mathbf{y}}), \tag{17.26}$$

$$\mathbf{F} = -\varepsilon\frac{e^{-j\beta r}}{4\pi r}(-I_y^E\hat{\mathbf{x}} + I_x^E\hat{\mathbf{y}}). \tag{17.27}$$

The integrals in the above expressions can be explicitly written for the case $\hat{\mathbf{n}} \equiv \hat{\mathbf{z}}$ in spherical coordinates, bearing in mind that the source-point position on the aperture is $\mathbf{r}' = x'\hat{\mathbf{x}} + y'\hat{\mathbf{y}}$:

$$I_x^E(\theta,\varphi)=\iint_{S_A} E_{a_x}(x',y')e^{j\beta(x'\sin\theta\cos\varphi+y'\sin\theta\sin\varphi)}dx'dy', \tag{17.28}$$

$$I_y^E(\theta,\varphi)=\iint_{S_A} E_{a_y}(x',y')e^{j\beta(x'\sin\theta\cos\varphi+y'\sin\theta\sin\varphi)}dx'dy', \tag{17.29}$$

$$I_x^H(\theta,\varphi)=\iint_{S_A} H_{a_x}(x',y')e^{j\beta(x'\sin\theta\cos\varphi+y'\sin\theta\sin\varphi)}dx'dy', \tag{17.30}$$

$$I_y^H(\theta,\varphi)=\iint_{S_A} H_{a_y}(x',y')e^{j\beta(x'\sin\theta\cos\varphi+y'\sin\theta\sin\varphi)}dx'dy'. \tag{17.31}$$

Note that the above integrals can be viewed as 2-D Fourier transforms of the aperture field components where x transforms into $\beta_x=-\beta\sin\theta\cos\varphi$ and y transforms into $\beta_y=-\beta\sin\theta\sin\varphi$.

The transverse components of the magnetic vector potential **A** in spherical terms are obtained from (17.26) as

$$A_\theta=\mu\frac{e^{-j\beta r}}{4\pi r}\left(-I_y^H\cdot\cos\theta\cos\varphi+I_x^H\cdot\cos\theta\sin\varphi\right), \tag{17.32}$$

$$A_\varphi=\mu\frac{e^{-j\beta r}}{4\pi r}\left(I_y^H\cdot\sin\varphi+I_x^H\cdot\cos\varphi\right), \tag{17.33}$$

which can also be written in the vector form:

$$\mathbf{A}_\perp=\mu\frac{e^{-j\beta r}}{4\pi r}\left[\hat{\boldsymbol{\theta}}\cos\theta(I_x^H\sin\varphi-I_y^H\cos\varphi)+\hat{\boldsymbol{\varphi}}(I_x^H\cos\varphi+I_y^H\sin\varphi)\right]. \tag{17.34}$$

Analogously,

$$\mathbf{F}_\perp=-\varepsilon\frac{e^{-j\beta r}}{4\pi r}\left[\hat{\boldsymbol{\theta}}\cos\theta(I_x^E\sin\varphi-I_y^E\cos\varphi)+\hat{\boldsymbol{\varphi}}(I_x^E\cos\varphi+I_y^E\sin\varphi)\right]. \tag{17.35}$$

By substituting the above expressions in (17.16), we obtain the far-zone **E** field:

$$E_\theta^{\text{far}}=j\beta\frac{e^{-j\beta r}}{4\pi r}\left[I_x^E\cos\varphi+I_y^E\sin\varphi+\eta\cos\theta\cdot(I_y^H\cos\varphi-I_x^H\sin\varphi)\right], \tag{17.36}$$

$$E_\varphi^{\text{far}}=j\beta\frac{e^{-j\beta r}}{4\pi r}\left[-\eta(I_x^H\cos\varphi+I_y^H\sin\varphi)+\cos\theta\cdot(I_y^E\cos\varphi-I_x^E\sin\varphi)\right]. \tag{17.37}$$

For apertures mounted on a flat conducting plane (e.g., slot antennas), the preferred equivalent model is the one using an electric wall with doubled magnetic current density,

$$\mathbf{M}_s = 2(\mathbf{E}_a \times \hat{\mathbf{n}}), \tag{17.38}$$

which is non-zero only in the slot, and it radiates in open space. This is because, in this case, the tangential **E**-field on the aperture is indeed zero everywhere except in the slot. The solution (valid only for $z \geq 0$), uses the fact that $\mathbf{I}^H = 0$ and the far-zone field is given by

$$E_\theta^{\text{far}}(\theta,\varphi) = j\beta \frac{e^{-j\beta r}}{4\pi r}\left(I_x^E \cos\varphi + I_y^E \sin\varphi\right), \tag{17.39}$$

$$E_\varphi^{\text{far}}(\theta,\varphi) = j\beta \frac{e^{-j\beta r}}{4\pi r}\cos\theta\left(I_y^E \cos\varphi - I_x^E \sin\varphi\right). \tag{17.40}$$

For apertures illuminated from open space (e.g., reflector antennas), the dual current formulation is used. Then, the usual assumption is that the aperture field resembles that of a locally-plane wave, i.e.,

$$\mathbf{H}_a = \hat{\mathbf{z}} \times \mathbf{E}_a / \eta. \tag{17.41}$$

This implies that

$$\mathbf{I}^H = \frac{1}{\eta}\hat{\mathbf{z}} \times \mathbf{I}^E \text{ or } I_x^H = -\frac{I_y^E}{\eta},\ I_y^H = \frac{I_x^E}{\eta}. \tag{17.42}$$

This assumption is valid for apertures that are at least a couple of wavelengths in extent where the reflector is in the far zone of the primary illuminating antenna. Then, (17.36)-(17.37) reduce to

$$E_\theta^{\text{far}}(\theta,\varphi) = j\beta \frac{e^{-j\beta r}}{4\pi r}\frac{(1+\cos\theta)}{2}\left(I_x^E \cos\varphi + I_y^E \sin\varphi\right), \tag{17.43}$$

$$E_\varphi^{\text{far}}(\theta,\varphi) = j\beta \frac{e^{-j\beta r}}{4\pi r}\frac{(1+\cos\theta)}{2}\left(I_y^E \cos\varphi - I_x^E \sin\varphi\right). \tag{17.44}$$

Compare (17.43)-(17.44) to (17.39)-(17.40). The terms in the brackets are identical. If the aperture has high gain, the factors containing $\cos\theta$ are not going to affect the pattern significantly, since $\cos\theta \approx 1$ within the main beam, and the two sets of formulas are going to be nearly equivalent.

5. The Uniform Rectangular Aperture in an Infinite Ground Plane

A rectangular aperture is defined in the xy plane as shown below.

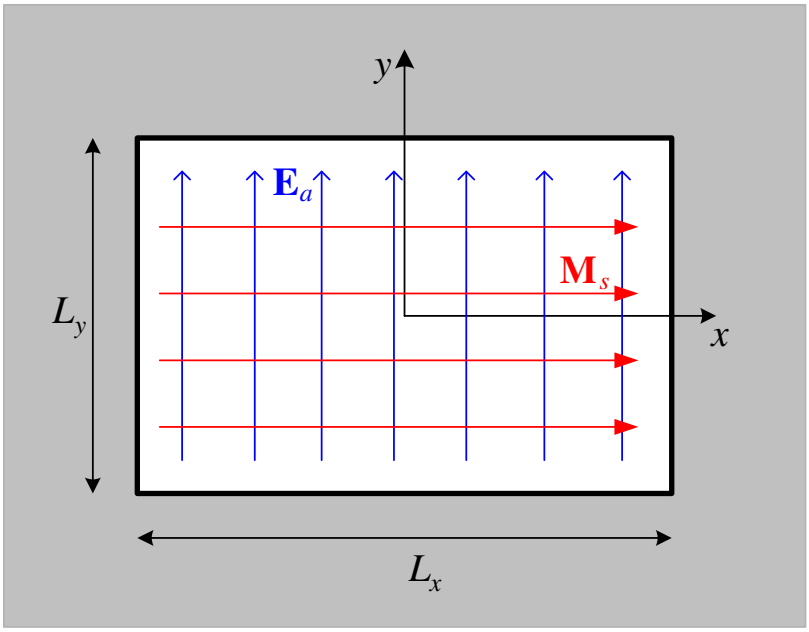

If the field is uniform in amplitude and phase across the aperture, it is referred to as a ***uniform rectangular aperture***. Let us assume that the aperture field is y-polarized:

$$\mathbf{E}_a = E_0\hat{\mathbf{y}},\ \text{for}\ |x| \le \frac{L_x}{2}\ \ \text{and}\ \ |y| \le \frac{L_y}{2},$$
$$\mathbf{E}_a = 0,\ \text{elsewhere}\ . \tag{17.45}$$

Using the equivalence principle, let us assume an electric wall at $z = 0$, where the equivalent magnetic current density is given by $\mathbf{M}_{s,e} = \mathbf{E}_0 \times \hat{\mathbf{n}}$. Applying image theory, we double the equivalent source radiating in open space:

$$\mathbf{M}_s = 2\mathbf{M}_{s,e} = 2(E_0\hat{\mathbf{y}}) \times \hat{\mathbf{z}} = 2E_0\hat{\mathbf{x}}\ \text{for}\ |x| \le \frac{L_x}{2}\ \ \text{and}\ \ |y| \le \frac{L_y}{2},.$$
$$\mathbf{M}_s = 0,\ \text{elsewhere.} \tag{17.46}$$

The only non-zero radiation integral is [see (17.29)]

$$I_y^E(\theta,\varphi) = 2E_0 \int_{-L_x/2}^{L_x/2} e^{j\beta x' \sin\theta\cos\varphi} dx' \cdot \int_{-L_y/2}^{L_y/2} e^{j\beta y' \sin\theta\sin\varphi} dy', \tag{17.47}$$

the solution of which yields

$$I_y^E(\theta,\varphi) = 2E_0 L_x L_y \frac{\sin\left(\frac{\beta L_x}{2}\sin\theta\cos\varphi\right)}{\left(\frac{\beta L_x}{2}\sin\theta\cos\varphi\right)} \cdot \frac{\sin\left(\frac{\beta L_y}{2}\sin\theta\sin\varphi\right)}{\left(\frac{\beta L_y}{2}\sin\theta\sin\varphi\right)}. \qquad (17.48)$$

To shorten the notations, let us introduce the *pattern variables*:

$$\begin{cases} u(\theta,\varphi) = 0.5\beta L_x \sin\theta\cos\varphi, \\ v(\theta,\varphi) = 0.5\beta L_y \sin\theta\sin\varphi\ . \end{cases} \qquad (17.49)$$

The complete radiation field is found by substituting (17.48) in (17.39)-(17.40):

$$\begin{cases} E_\theta(\theta,\varphi) = j\beta\frac{e^{-j\beta r}}{2\pi r} E_0 L_x L_y \sin\varphi \cdot \left(\frac{\sin u}{u}\right)\left(\frac{\sin v}{v}\right), \\ E_\varphi(\theta,\varphi) = j\beta\frac{e^{-j\beta r}}{2\pi r} E_0 L_x L_y \cos\theta\cdot\cos\varphi \cdot \left(\frac{\sin u}{u}\right)\left(\frac{\sin v}{v}\right). \end{cases} \qquad (17.50)$$

The total-field amplitude pattern is, therefore,

$$\begin{aligned} |\,\overline{E}(\theta,\varphi)\,| = F(\theta,\varphi) &= \sqrt{\sin^2\varphi + \cos^2\theta\cos^2\varphi}\cdot\left(\frac{\sin u}{u}\right)\left(\frac{\sin v}{v}\right) = \\ &= \sqrt{1-\sin^2\theta\cos^2\varphi}\cdot\left(\frac{\sin u}{u}\right)\left(\frac{\sin v}{v}\right). \end{aligned} \qquad (17.51)$$

The principal plane patterns are:

<u>*E*-plane pattern</u> $\underline{(\varphi = \pi/2)}$

$$F(\theta) = \overline{E}_\theta(\theta) = \frac{\sin\left(0.5\beta L_y \sin\theta\right)}{\left(0.5\beta L_y \sin\theta\right)},\ \overline{E}_\varphi = 0 \qquad (17.52)$$

<u>*H*-plane pattern</u> $\underline{(\varphi = 0)}$

$$F(\theta) = \overline{E}_\varphi(\theta) = \cos\theta\cdot\frac{\sin\left(0.5\beta L_x \sin\theta\right)}{\left(0.5\beta L_x \sin\theta\right)},\ \overline{E}_\theta = 0 \qquad (17.53)$$

Notice that the aperture yields a linearly polarized far field in all directions. In the *E*-plane, the field is polarized along θ, whereas in the *H*-plane, it is polarized along φ.

PRINCIPLE PATTERNS FOR APERTURE OF SIZE: $L_x = 3\lambda,\ L_y = 2\lambda$

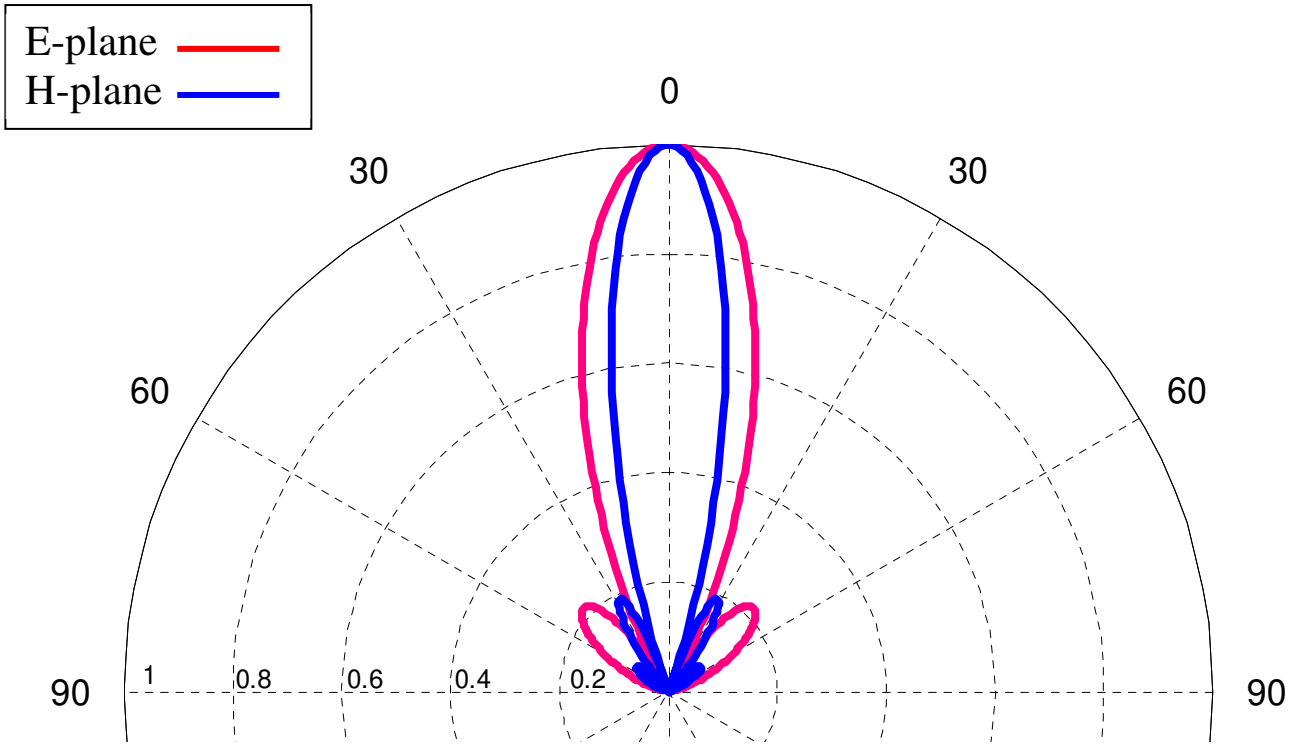

For electrically large apertures, the main beam is narrow and the $(1-\sin^2\theta\cos^2\varphi)^{1/2}$ in (17.51) is roughly equal to 1 for all observation angles within the main beam. That is why, in the theory of large apertures and arrays, it is assumed that the amplitude pattern is simply

$$f(u,v) \approx \left| \frac{\sin u}{u} \cdot \frac{\sin v}{v} \right|, \qquad (17.54)$$

where $u = 0.5\beta L_x \sin\theta\cos\varphi$ and $v = 0.5\beta L_y \sin\theta\sin\varphi$ as defined in (17.49).

Below is a view of the $|(\sin u)/u|$ function for $L_x = 20\lambda$ and $\varphi = 0°$ (*H*-plane pattern):

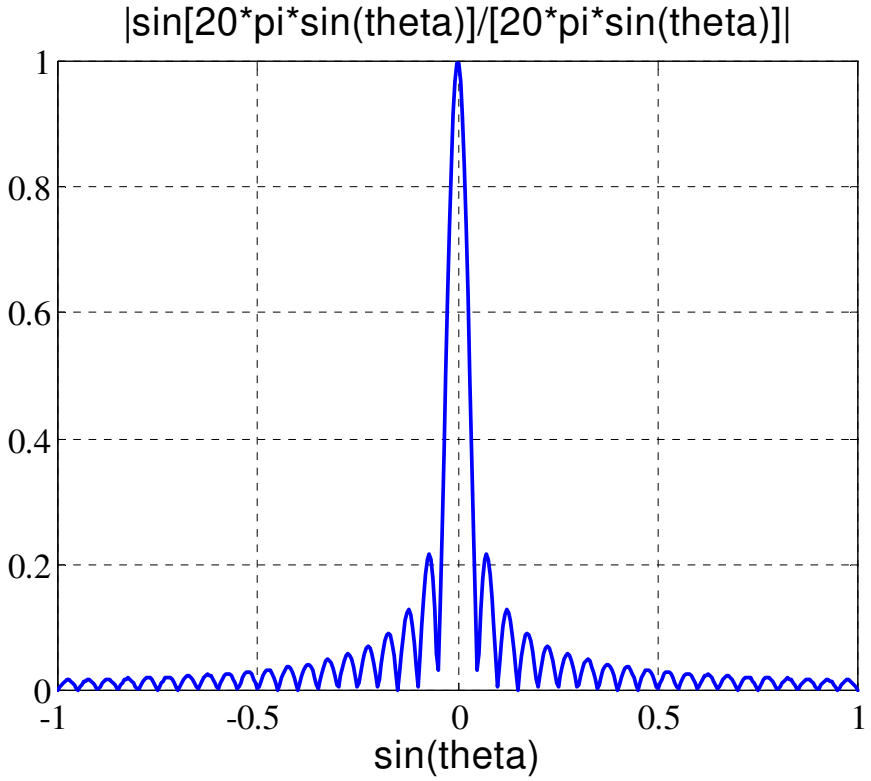

Here is a view of the $|\sin v / v|$ function for $L_y = 10\lambda$ and $\varphi = 90°$ (E-plane pattern):

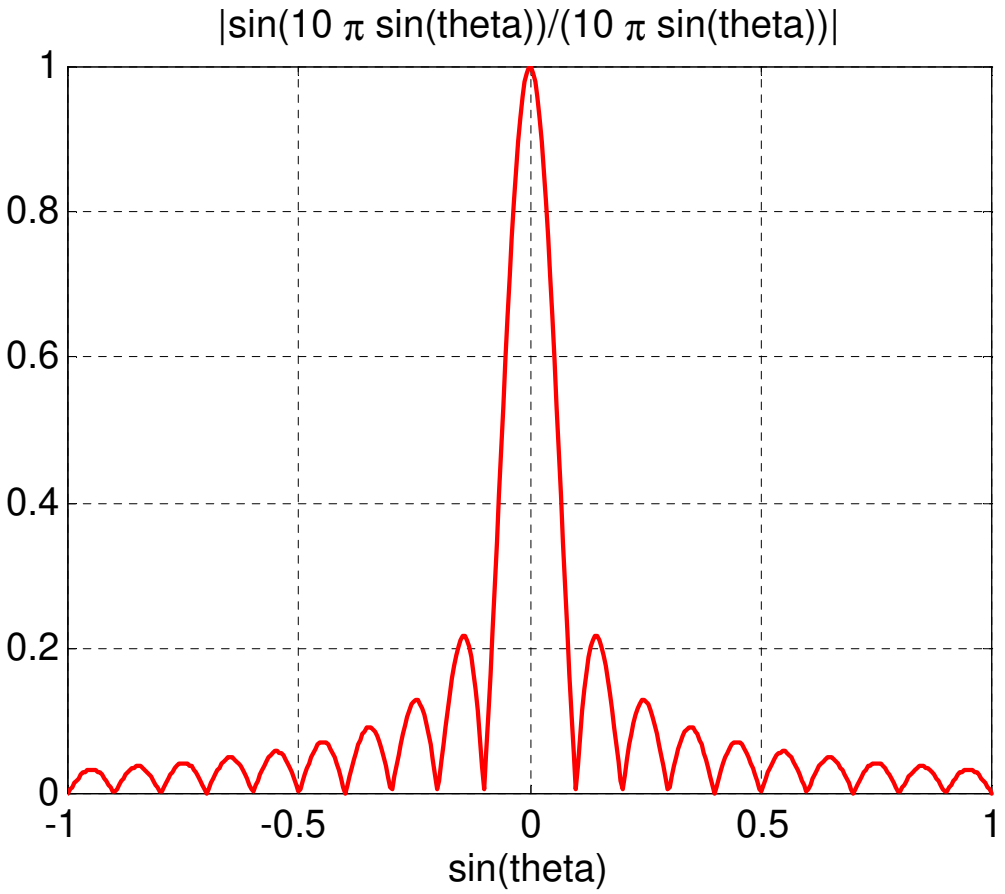

Notice that the side-lobe level in both patterns is the same although the size of the aperture is different in the x and y directions ($L_x = 20\lambda$, $L_y = 10\lambda$). This is due to the first minor maximum of the function $|\sin u / u| \approx 0.2172$ occuring at $u \approx 4.494$. The value of this maximum does not depend on the size of the aperture as long as this size exceeds a wavelength.[2]

Point for Discussion: The field of a narrow slot (a slit) ($L_y \ll \lambda$).

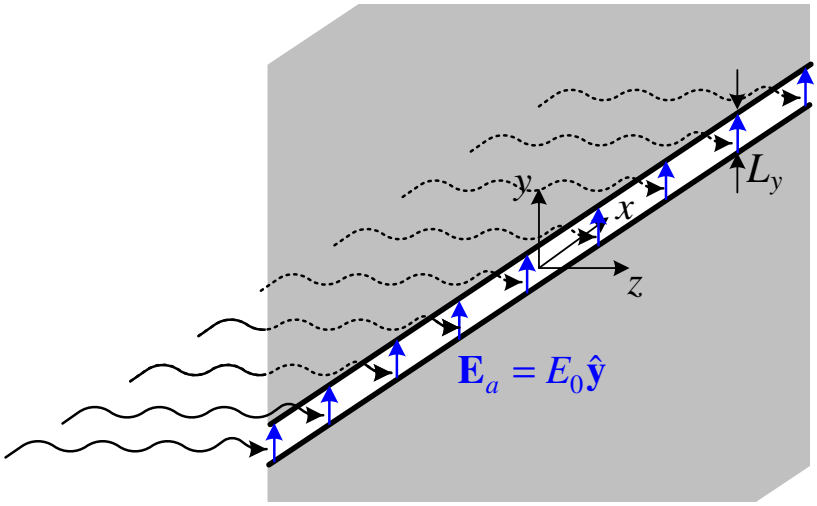

The radiation integral for the case of a slit is a particular case of (17.48):

$$\left(I_y^E\right)_{\text{slit}} = 2E_0 L_x L_y \frac{\sin\left(0.5\beta L_x \sin\theta\cos\varphi\right)}{\left(0.5\beta L_x \sin\theta\cos\varphi\right)} \cdot \underbrace{\lim_{L_y\to 0}\left[\frac{\sin\left(0.5\beta L_y \sin\theta\sin\varphi\right)}{\left(0.5\beta L_y \sin\theta\sin\varphi\right)}\right]}_{1}, \quad (17.55)$$

which leads to

$$\left(I_y^E\right)_{\text{slit}} = 2E_0 L_x L_y \frac{\sin\left(0.5\beta L_x \sin\theta\cos\varphi\right)}{\left(0.5\beta L_x \sin\theta\cos\varphi\right)}. \quad (17.56)$$

The total field pattern of the slit is then

$$F(\theta,\varphi) = \sqrt{1-\sin^2\theta\cos^2\varphi}\left[\frac{\sin\left(0.5\beta L_x \sin\theta\cos\varphi\right)}{0.5\beta L_x \sin\theta\cos\varphi}\right], \quad (17.57)$$

whereas the principal plane 2D patterns follow from (17.52) and (17.53) as

[2] The first minor maximum of the *sinc* function's absolute value is reached when its argument solves the transcendental equation $\tan x = x$.

shown below.

- *E*-plane pattern ($\varphi = \pi/2$, yz plane) is omnidirectional:

$$F(\theta) = \bar{E}_\theta(\theta) = \lim_{L_y \to 0} \left[\frac{\sin\left(0.5\beta L_y \sin\theta\right)}{\left(0.5\beta L_y \sin\theta\right)} \right] = 1. \tag{17.58}$$

- *H*-plane pattern ($\varphi = 0$, xz plane)

$$F(\theta) = \bar{E}_\varphi = |\cos\theta| \cdot \left| \frac{\sin\left(0.5\beta L_x \sin\theta\right)}{\left(0.5\beta L_x \sin\theta\right)} \right| \tag{17.59}$$

Beamwidths of Uniform Rectangular Aperture in a Ground Plane

(a) First-null beamwidth (FNBW)

We need the locations of the first nulls in the pattern in order to calculate the FNBW. The nulls of the *E*-plane pattern are determined from (17.52) as

$$\frac{\beta L_y}{2} \sin\theta_{/\theta=\theta_n} = n\pi, \quad n = 1, 2, \ldots, \tag{17.60}$$

$$\Rightarrow \theta_n = \arcsin\left(\frac{n\lambda}{L_y}\right). \tag{17.61}$$

The first null occurs at $n = 1$.

$$\Rightarrow FNBW_E = 2\theta_n = 2\arcsin\left(\frac{\lambda}{L_y}\right). \tag{17.62}$$

In a similar fashion, $FNBW_H$ is determined as

$$FNBW_H = 2\arcsin\left(\frac{\lambda}{L_x}\right). \tag{17.63}$$

It is apparent that larger aperture widths lead to narrower beams.

(b) Half-power beamwidth (HPBW)

The half-power point in the *E*-plane occurs when

$$\frac{\sin\left(0.5\beta L_y \sin\theta\right)}{\left(0.5\beta L_y \sin\theta\right)} = \frac{1}{\sqrt{2}}, \tag{17.64}$$

or

$$0.5\beta L_y \sin\theta_{/\theta=\theta_h} \approx 1.391, \tag{17.65}$$

$$\Rightarrow \theta_h \approx \arcsin\left(\frac{0.443\lambda}{L_y}\right), \text{ rad}, \tag{17.66}$$

$$HPBW_E \approx 2\arcsin\left(\frac{0.443\lambda}{L_y}\right). \tag{17.67}$$

A first-order approximation is possible for very small arguments in (17.67), i.e., when $L_y \gg 0.443\lambda$ (large aperture):

$$HPBW_E \approx 0.886\frac{\lambda}{L_y}. \tag{17.68}$$

The half-power beamwidth in the *H*-plane is analogous:

$$HPBW_H \approx 2\arcsin\left(\frac{0.443\lambda}{L_x}\right). \tag{17.69}$$

Side-lobe level of Uniform Rectangular Aperture in a Ground Plane

It is obvious from the properties of the $|\sin x / x|$ function that the first side lobe has the largest maximum of all side lobes. In the *E*-plane, the side-love level is

$$|E_\theta(\theta=\theta_s)| \approx \left|\frac{\sin 4.494}{4.494}\right| \approx 0.217 \approx -13.26, \text{ dB}. \tag{17.70}$$

When evaluating all side-lobe levels and beamwidths, especially in the *H*-plane, one must include the $\cos\theta$ factor as well. The larger the aperture, the less important this factor is.

Directivity of Uniform Rectangular Aperture in a Ground Plane

The antenna solid angle Ω_A is needed to calculate the directivity from

$$D_0 = 4\pi / \Omega_A. \tag{17.71}$$

The radiation intensity in any direction can be expressed through the normalized field pattern as

$$U(\theta,\varphi) = U_{\max}[\bar{F}(\theta,\varphi)]^2. \tag{17.72}$$

The far-field pattern $\bar{F}(\theta,\varphi)$ is available from (17.51), namely,

$$F(\theta,\varphi) = \sqrt{1-\sin^2\theta\cos^2\varphi}\cdot\left(\frac{\sin u}{u}\right)\left(\frac{\sin v}{v}\right). \tag{17.73}$$

The antenna solid angle is then calculated as

$$\Omega_A = \int_0^{2\pi}\int_0^{\pi/2}[F(\theta,\varphi)]^2\sin\theta d\theta d\varphi, \tag{17.74}$$

which, in turn, is used to compute the directivity from (17.71).

However, with an aperture illuminated by a TEM wave, we can use a simpler approach. Generally, for slot and reflector (dish) antennas, the assumption of a TEM wave at the aperture is quite accurate. Then, if $\mathbf{E} = \hat{\mathbf{y}}E_0$,

$$\mathbf{H}_a = -\hat{\mathbf{x}}E_0/\eta, \tag{17.75}$$

where η is the intrinsic impedance of the medium. Analogous expression is used for an open-end waveguide antennas where η is replaced by the waveguide's wave impedance Z_w. The far-field components in this case were already derived in (17.43) and (17.44). They lead to the following radiation intensity:

$$U(\theta,\varphi) = \frac{\beta^2}{32\pi^2\eta}(1+\cos\theta)^2\left(|I_x^E(\theta,\varphi)|^2 + |I_y^E(\theta,\varphi)|^2\right). \tag{17.76}$$

The maximum value of the function in (17.76) is derived after substituting the radiation integrals from (17.28) and (17.29), which leads to

$$U_{\max} = \frac{\beta^2}{8\pi^2\eta}\left|\iint_{S_A}\mathbf{E}_a ds'\right|^2. \tag{17.77}$$

The integration of the radiation intensity (17.76) over a closed sphere is not easy. It can be avoided by observing that the total power reaching the far zone must have passed through the aperture in the first place. In an aperture, where the field obeys (17.75), this power is determined as

$$\Pi = \oiint_S \mathbf{P}_{av} \cdot d\mathbf{s} = \frac{1}{2\eta} \iint_{S_A} |\, \mathbf{E}_a \,|^2 \, ds \,. \tag{17.78}$$

Substituting (17.77) and (17.78) into (17.71) finally yields

$$D_0 = \frac{4\pi}{\lambda^2} \times \boxed{\frac{\left| \iint_{S_A} \mathbf{E}_a ds' \right|^2}{\iint_{S_A} |\, \mathbf{E}_a \,|^2 \, ds'}} \,. \tag{17.79}$$

A_{eff}

In the case of a ***uniform rectangular aperture***,

$$\Pi = L_x L_y \frac{|\, E_0 \,|^2}{2\eta} \,, \tag{17.80}$$

$$U_{\max} = \left(\frac{L_x L_y}{\lambda} \right)^2 \frac{|\, E_0 \,|^2}{2\eta} \,. \tag{17.81}$$

Thus, the directivity is found to be

$$D_0 = 4\pi \frac{U_{\max}}{\Pi} = \frac{4\pi}{\lambda^2} L_x L_y = \frac{4\pi}{\lambda^2} A_p = \frac{4\pi}{\lambda^2} A_{eff} \,. \tag{17.82}$$

Note that ***the physical and effective areas of a uniform aperture are equal***.

6. The Uniform Rectangular Aperture in Open Space

Now the rectangular aperture is ***not*** mounted on a ground plane. The field distribution is the same as in (17.45) but now the **H** field must be defined, too, in order to apply the equivalence principle with both types of surface currents,

$$\left.\begin{aligned} \mathbf{E}_a &= \hat{\mathbf{y}} E_0 \\ \mathbf{H}_a &= -\hat{\mathbf{x}} E_0 / \eta \end{aligned}\right\}, \quad \begin{aligned} &-L_x / 2 \le x' \le L_x / 2 \\ &-L_y / 2 \le y' \le L_y / 2. \end{aligned} \tag{17.83}$$

Note that (17.83) implies an assumption that $\mathbf{E}_a$ and $\mathbf{H}_a$ relate through the medium intrinsic impedance η like in a TEM traveling wave.

To form the equivalent problem, an infinite surface is chosen to extend in the $z = 0$ plane. Over the entire surface, the equivalent $\mathbf{J}_s$ and $\mathbf{M}_s$ surface currents must be defined. Both $\mathbf{J}_s$ and $\mathbf{M}_s$ are not really zero outside the aperture in the $z = 0$ plane because the respective tangential field is not zero. Moreover, the field

is ***not known*** *a priori* outside the aperture. Thus, an exact equivalent problem cannot be built.

The simplest approximation is that $\mathbf{E}_a$ and $\mathbf{H}_a$ are zero outside the aperture in the $z=0$ plane, i.e., $\mathbf{E}_a = 0, \mathbf{H}_a = 0$ for $|x'| > L_x$ and $|y'| > L_y$. Then, the equivalent currents $\mathbf{J}_s$ and $\mathbf{M}_s$ are defined as:

$$\left.\begin{aligned} \mathbf{M}_s &= -\hat{\mathbf{n}} \times \mathbf{E}_a = \underbrace{-\hat{\mathbf{z}} \times \hat{\mathbf{y}}}_{\hat{\mathbf{x}}} E_0 \\ \mathbf{J}_s &= \hat{\mathbf{n}} \times \mathbf{H}_a = \underbrace{\hat{\mathbf{z}} \times (-\hat{\mathbf{x}})}_{-\hat{\mathbf{y}}} \frac{E_0}{\eta} \end{aligned}\right\} \text{ for } \begin{cases} -L_x/2 \le x' \le L_x/2 \\ -L_y/2 \le y' \le L_y/2 \end{cases} \tag{17.84}$$

$$\mathbf{J}_s = \mathbf{M}_s = 0 \text{ for } |x'| > L_x/2, \ |y'| > L_y$$

Since the equivalent currents are related via the impedance assumption (17.83), only the integral $I_y^E(\theta,\varphi)$ is needed for substitution in the far-field expressions (17.43)-(17.44). $I_y^E(\theta,\varphi)$ is the same as in (17.48), i.e.,

$$I_y^E(\theta,\varphi) = 2E_0 L_x L_y \frac{\sin\left(0.5\beta L_x \sin\theta\cos\varphi\right)}{\left(0.5\beta L_x \sin\theta\cos\varphi\right)} \cdot \frac{\sin\left(0.5\beta L_y \sin\theta\sin\varphi\right)}{\left(0.5\beta L_y \sin\theta\sin\varphi\right)}. \tag{17.85}$$

The far-field components are obtained by substituting (17.85) into (17.43) and (17.44):

$$\begin{aligned} E_\theta &= C\sin\varphi \frac{\left(1+\cos\theta\right)}{2} \frac{\sin u}{u} \frac{\sin v}{v}, \\ E_\varphi &= C\cos\varphi \frac{\left(1+\cos\theta\right)}{2} \frac{\sin u}{u} \frac{\sin v}{v}, \end{aligned} \tag{17.86}$$

where

$$C = j\beta L_x L_y E_0 \frac{e^{-j\beta r}}{2\pi r},$$

$$u = 0.5\beta L_x \sin\theta\cos\varphi,$$

$$v = 0.5\beta L_y \sin\theta\sin\varphi.$$

The far-field expressions in (17.86) are very similar to those of the aperture mounted on a ground plane, see (17.50). For small values of θ, the patterns of both apertures are practically identical.

An exact analytical evaluation of the directivity is difficult. However, according to the approximations made, the directivity formula derived in (17.79) should provide fairly accurate value. Thus, the directivity is the same as in the case of the aperture mounted on a ground plane.

7. The Tapered Rectangular Aperture on a Ground Plane

The uniform rectangular aperture has the maximum possible effective area (for an aperture-type antenna) equal to its physical area. This also implies that it has the highest possible directivity for all constant-phase excitations of a rectangular aperture. However, the directivity is not the only important factor in the design of an antenna. A factor that often is in conflict with the directivity is the side-lobe level (SLL). The uniform-distribution excitation produces the highest SLL of all constant-phase excitations of a rectangular aperture (≈ −13 dB). It is shown below that a reduction of the SLL can be achieved by tapering the equivalent sources distribution from a maximum at the aperture's center to zero values at its edges.

One practical aperture of tapered source distribution is the open rectangular waveguide. The dominant TE_{10} mode has the following distribution:

$$\mathbf{E}_a = \hat{\mathbf{y}} E_0 \cos\left(\frac{\pi}{L_x} x'\right), \quad \begin{cases} -L_x / 2 \le x' \le L_x / 2 \\ -L_y / 2 \le y' \le L_y / 2 \end{cases} \tag{17.87}$$

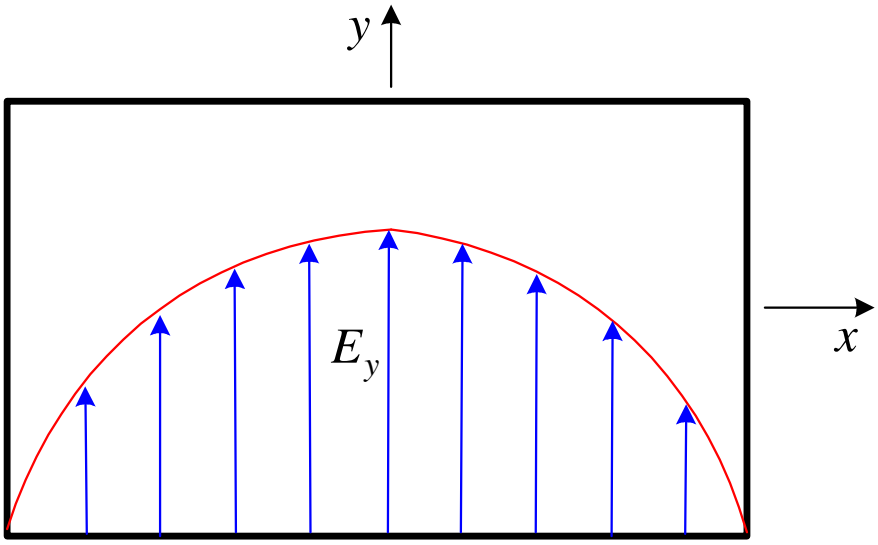

The general procedure for the far-field analysis is the same as before (Sections 5 and 6). The only difference is in the field distribution. Again, only the integral $I_y^E(\theta,\varphi)$ is evaluated:

$$I_y^E(\theta,\varphi)=2E_0\underbrace{\int_{-L_x/2}^{L_x/2}\cos\left(\frac{\pi}{L_x}x'\right)e^{j\beta x'\sin\theta\cos\varphi}dx'}_{\text{cosine distribution along } x}\cdot\underbrace{\int_{-L_y/2}^{L_y/2}e^{j\beta y'\sin\theta\sin\varphi}dy'}_{\text{constant distribution along } y}. \quad (17.88)$$

The integral of the y' variable was already solved in (17.47)-(17.48):

$$I_y(\theta,\varphi)=\int_{-L_y/2}^{L_y/2}e^{j\beta y'\sin\theta\sin\varphi}dy'=L_y\frac{\sin\left(0.5\beta L_y\sin\theta\sin\varphi\right)}{\left(0.5\beta L_y\sin\theta\sin\varphi\right)}. \quad (17.89)$$

The integral over the x' variable is also easily solved:

$$I_x(\theta,\varphi)=\int_{-L_x/2}^{L_x/2}\cos\left(\frac{\pi}{L_x}x'\right)e^{j\beta x'\sin\theta\cos\varphi}dx'=$$

$$=\int_{-L_x/2}^{L_x/2}\cos\left(\frac{\pi}{L_x}x'\right)\left[\cos\left(\beta x'\sin\theta\cos\varphi\right)+j\sin\left(\beta x'\sin\theta\cos\varphi\right)\right]dx'=$$

$$=\frac{1}{2}\int_{-L_x/2}^{L_x/2}\left\{\cos\left[\left(\frac{\pi}{L_x}-\beta\sin\theta\cos\varphi\right)x'\right]+\cos\left[\left(\frac{\pi}{L_x}+\beta\sin\theta\cos\varphi\right)x'\right]\right\}dx'+$$

$$+\frac{j}{2}\int_{-L_x/2}^{L_x/2}\left\{\sin\left[\left(\beta\sin\theta\cos\varphi-\frac{\pi}{L_x}\right)x'\right]+\cos\left[\left(\beta\sin\theta\cos\varphi+\frac{\pi}{L_x}\right)x'\right]\right\}dx'$$

$$\Rightarrow I_x(\theta,\varphi)=\frac{\pi L_x}{2}\frac{\cos\left(\frac{\beta L_x}{2}\sin\theta\cos\varphi\right)}{\left[\left(\frac{\pi}{2}\right)^2-\frac{\beta L_x}{2}\sin\theta\cos\varphi\right]} \quad (17.90)$$

The substitution of (17.89) and (17.90) in (17.88) leads to

$$I_y^E(\theta,\varphi)=\pi E_0 L_x L_y \frac{\cos\left(\underbrace{\frac{\beta L_x}{2}\sin\theta\cos\varphi}_{u(\theta,\varphi)}\right)}{\left[\left(\frac{\pi}{2}\right)^2-\left(\underbrace{\frac{\beta L_x}{2}\sin\theta\cos\varphi}_{u(\theta,\varphi)}\right)^2\right]}\times\frac{\sin\left[\underbrace{\frac{\beta L_y}{2}\sin\theta\sin\varphi}_{v(\theta,\varphi)}\right]}{\left(\underbrace{\frac{\beta L_y}{2}\sin\theta\sin\varphi}_{v(\theta,\varphi)}\right)} \tag{17.91}$$

To derive the far-field components, (17.91) is substituted in (17.36)-(17.37):

$$\begin{aligned} E_\theta(\theta,\varphi)&=-\frac{\pi}{2}C\sin\varphi\cdot\frac{\cos u}{\left[u^2-\left(\frac{\pi}{2}\right)^2\right]}\cdot\frac{\sin v}{v}\\ E_\varphi(\theta,\varphi)&=-\frac{\pi}{2}C\cos\theta\cos\varphi\cdot\frac{\cos u}{\left[u^2-\left(\frac{\pi}{2}\right)^2\right]}\cdot\frac{\sin v}{v} \end{aligned} \tag{17.92}$$

where

$$C=j\beta L_x L_y E_0\frac{e^{-j\beta r}}{2\pi r},$$
$$u=0.5\beta L_x\sin\theta\cos\varphi,$$
$$v=0.5\beta L_y\sin\theta\sin\varphi.$$

Principle plane patterns

In the *E*-plane, the aperture is not tapered. As expected, the *E*-plane principal pattern is the same as that of a uniform aperture.

E-plane ($\varphi=90^\circ$):

$$F(\theta)=\overline{E}_\theta(\theta)=\frac{\sin\left(\frac{\beta L_y}{2}\sin\theta\right)}{\left(\frac{\beta L_y}{2}\sin\theta\right)} \tag{17.93}$$

H-plane ($\varphi = 0^\circ$):

$$F(\theta) = \bar{E}_\varphi(\theta) = \cos\theta \cdot \frac{\cos\left(\frac{\beta L_x}{2}\sin\theta\right)}{\left(\frac{\beta L_x}{2}\sin\theta\right)^2 - \left(\frac{\pi}{2}\right)^2}. \qquad (17.94)$$

H-PLANE PATTERN – UNIFORM VS. TAPERED ILLUMINATION ($L_x = 3\lambda$):

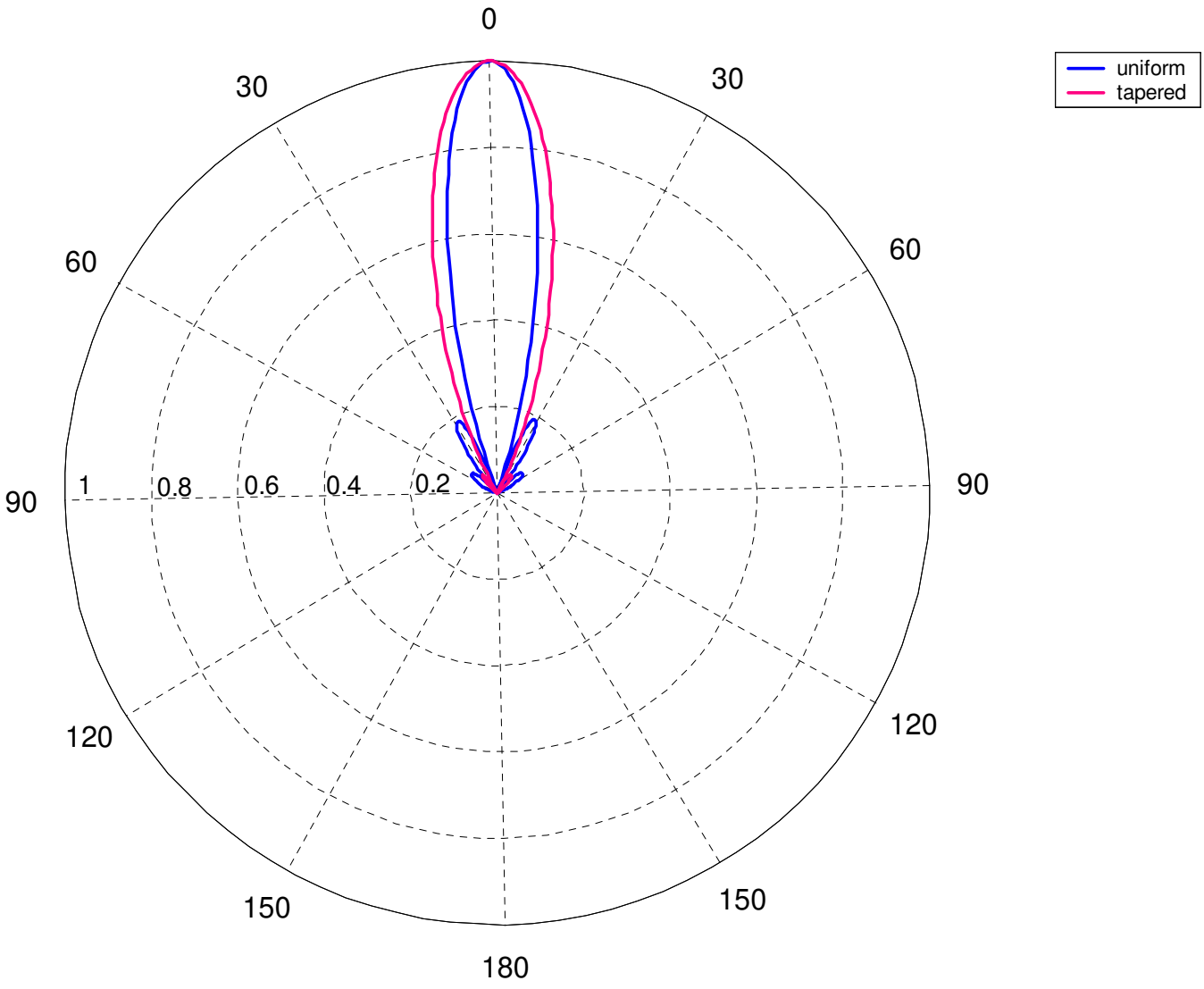

The lower SLL of the tapered-source pattern is obvious. It is better seen in the rectangular plot given below. The price to pay for the lower SLL is the decrease in directivity (the beamwidth of the major lobe increases).

H-PLANE PATTERN RECTANGULAR PLOT – UNIFORM VS. TAPERED ILLUMINATION WHEN $L_x = 3\lambda$

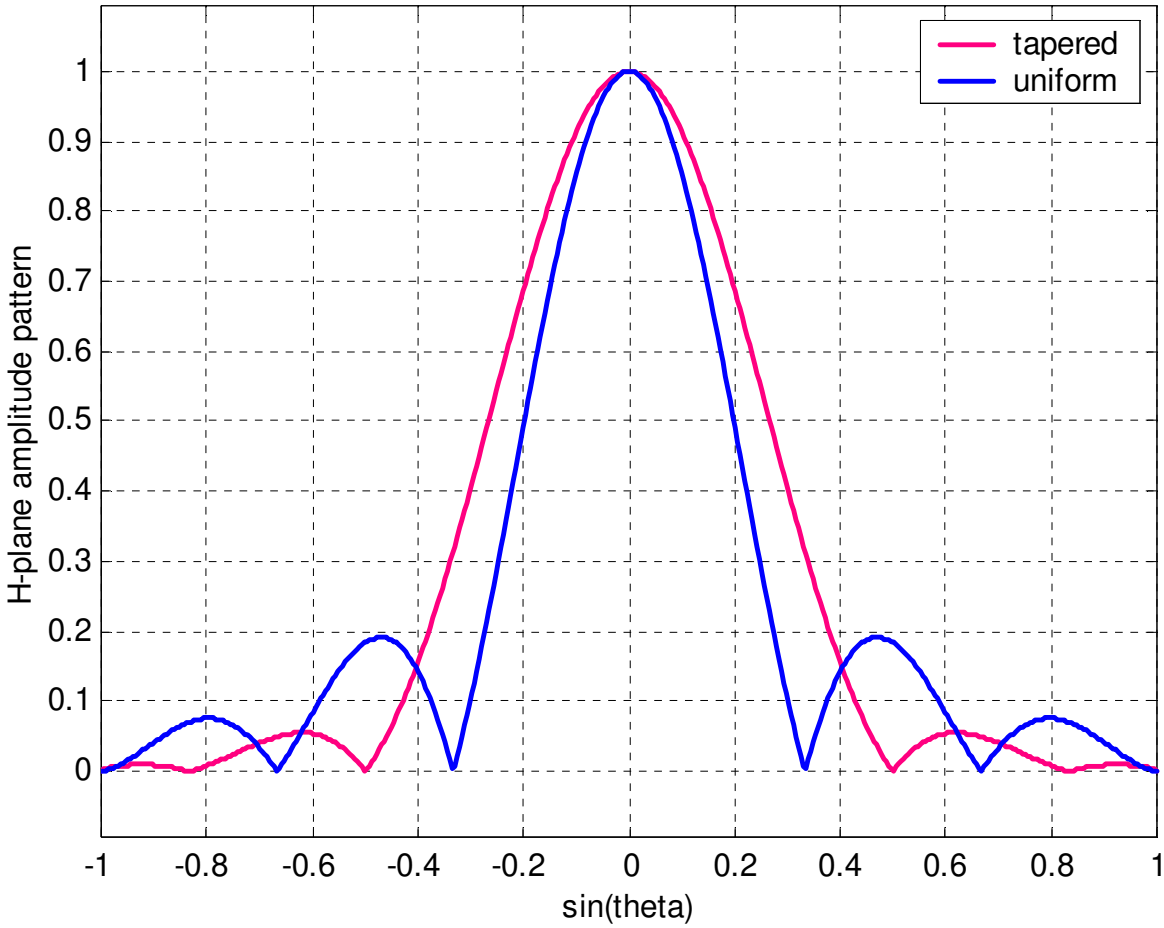

The above example of $L_x = 3\lambda$ illustrates well the effect of source distribution on the far-field pattern. However, a more practical example is the rectangular-waveguide open-end aperture, where the waveguide operates in a dominant mode, i.e. $\lambda_0 / 2 < L_x < \lambda_0$. Here, λ_0 is the wavelength in open space. Consider the case $L_x = 0.75\lambda_0$. The principal-plane patterns for an aperture on a ground plane look like this:

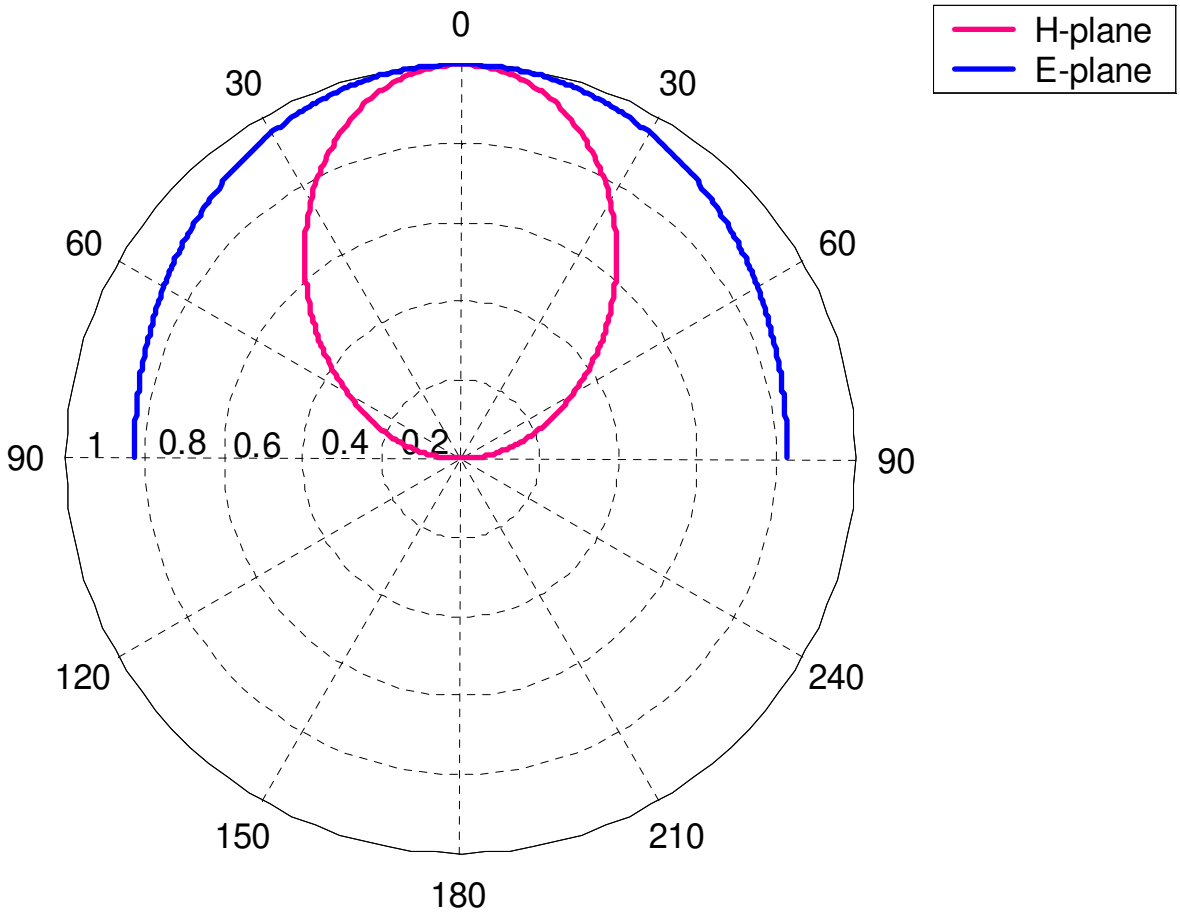

In the plot above, the polar patterns are shown for an X-band waveguide of cross-section defined by $L_x = 2.286$ cm, $L_y = 1.016$ cm. The frequency $f_0 = 9.84$ GHz is considered when the free-space wavelength is $\lambda_0 = 3.048$ cm.

The case of a dominant-mode open-end waveguide radiating in free space can be analyzed following the approaches outlined in this Section and in Section 6. The calculation of the beamwidths and the directivity is analogous to the previous cases. Only the final results will be given here for the case of the x-tapered (cosine taper) aperture on a ground plane.

$$\underline{\text{Directivity}}: \; D_0 = \frac{4\pi}{\lambda^2} \cdot \frac{8}{\pi^2} L_x L_y \tag{17.95}$$

$$\underline{\text{Effective area}}: \; A_{eff} = \frac{8}{\pi^2} L_x L_y \approx 0.81 \cdot A_p \tag{17.96}$$

Note the decrease in the directivity and the effective area compared to the uniform-aperture case.

Half-power beamwidths:

$$HPBW_E = \frac{50.6}{L_y / \lambda}, \text{ deg. } (= HPBW_E \text{ of the uniform aperture}) \quad (17.97)$$

$$HPBW_H = \frac{68.8}{L_x / \lambda}, \text{ deg. } (> HPBW_H \text{ of the uniform aperture}) \quad (17.98)$$

The above results are approximate. Better results are obtained if the following factors are taken into account:

- the phase constant of the waveguide β_g and its wave impedance Z_w are not equal to the free-space phase constant $\beta_0 = \omega\sqrt{\mu_0\varepsilon_0}$ and intrinsic impedance $Z_0 = \sqrt{\mu_0 / \varepsilon_0}$; they are dispersive;
- the abrupt termination at the waveguide open end introduces reflection, which affects the field at the aperture;
- there are strong fringe currents at the waveguide walls, which contribute to the overall radiation.